JOURNAL OF APPLIED ELECTROCHEMISTRY **28** (1998) 601–606

Hydrogen activation of spectroscopic graphite surface by argon plasma etching

P. DABO, L. BROSSARD*, H. MÉNARD, P. TREMBLAY

*Centre de recherche en Électrochimie et Électrocatalyse, Département de Chimie, Université de Sherbrooke, Sherbrooke, Québec, Canada JIK 2R1 and *Institut de recherche d'Hydro-Québec, 1800 Boul. Lionel Boulet, Varennes, Québec, Canada J3X 1S1*

Received 9 January 1997; revised 11 July 1997

Argon plasma bombardment was successfully used for the hydrogen activation of spectroscopic graphite electrodes. The hydrogen evolution reaction (HER) in 1 M KOH was investigated using electrochemical techniques such as galvanostatic polarization and a.c. impedence spectroscopy; the electrode surface was characterized by SEM. It is shown that the rate of HER at a given hydrogen overpotential value increases exponentially with the etching time (ET), up to ETs of 30 min, and slightly decreases from 30 to 60 min. The double-layer capacity (C_{dl}) was established against the hydrogen overpotential for different ETs, with C_{dl} reaching its maximum for ETs of 30 min. Moreover, it is shown that the etching process also leads to a significant increase in intrinsic activity toward HER.

Keywords: *a.c. impedence spectroscopy*, *argon plasma etching*, *graphite electrodes*, *hydrogen evolution*

1. Introduction

Carbon is used extensively in electrochemistry due to its numerous advantages, for example, it is relatively inert chemically in many electrolytes. However, in many applications, carbon electrodes suffer from poor activity. To overcome this problem, many attempts have been made to improve the surface properties. Some common techniques include: mechanical polishing [1, 2], chemical [3], thermal [4] and electrochemical [5] treatments, laser irradiation [6], ion sputtering oxidation [7], and radio frequency plasma [8]. Various explanations have been proposed for the carbon electrode activation processes, such as the removal of possible contaminants from the electrode surface [5], the increase of the surface roughness factor and the exposure of fresh edges planes, microparticles, and defects that may be ideal sites for electron transfer [9].

The effect of ion bombardment on highly oriented pyrolytic graphite (HOPG) surfaces has recently been investigated by a.c. electrochemical impedance spectroscopy in relation to the hydrogen evolution reaction (HER) [10]. It has been shown that the double-layer capacitance of the electrodes increases almost linearly with the etching time as a result of the formation of cone-like peaks on the electrode surface.

The present investigation deals with the effect of argon plasma etching on the spectroscopic graphite surface in relation to the HER in 1 M KOH aqueous solution of 25 °C. Spectroscopic graphite, which is widely used in arc or spark emission spectroscopy, provides a convenient material for solid electrodes. Its high purity makes its use very attractive for electrocatalysis applications. Special attention was paid to the effect of the etching time (ET) on the surface characteristics and the applied current and pressure for sustaining the argon plasma on the HER were also taken into account.

Activated spectroscopic graphite electrodes using etching process are considered possible candidates for the electrocatalytic hydrogenation of organic compounds, since carbon materials have ideal characteristics for this type of electrochemistry [11, 12].

2. Experimental details

2.1. *Electrodes preparation*

Crystal parameters of spectroscopic graphite rods (Graf Spec, Spectrex Ltd) determined from XRD measurements using a Rigaku D/MaxB diffractometer are presented in Table 1. The mean size of the graphitic microcrystallite along the *a*-axis, L_a, and the mean size of the graphitic microcrystallite along the *c*-axis, L_c, are both calculated using the Scherrer equation [13]. The values of d_{002}, L_a and L_c are characteristics of randomly oriented graphite [6], which means a graphitized carbon with randomly oriented graphite microcrystallites, which is different from an amorphous carbon.

Spectroscopic graphite rods (0.3 cm^2 of geometric surface area) were cut to obtain pellets approximately 0.5 cm in length. The samples were mechanically polished with a sequence of smaller particle-size

0021-891X

Table 1. Crystal parameters of a spectroscopic graphite surface

	d_{002}* nm	L_a† nm	L_c‡ nm
Spectroscopic graphite	0.336	14.0	15.5

* d_{002}: interplanar spacing.
† mean size of graphitic microcrystallite along *a*-axis.
‡ mean size of graphitic microcrystallite along *c*-axis.

abrasive powders (silicon carbide): 200, 400 and 600. After each polishing steps, the sample was rinsed with triply deionized water and dried by forced air convection. Immediately after, the pellet was placed in a plasma-etching chamber, (Hummer VI Sputter Coating); the pressure in the chamber was lowered to 50 mtorr. High-purity argon (99.998%) was then introduced in the chamber via a micrometric admittance valve. For the first set of experiments, the pressure, which was measured with a Pirani gauge, was stabilized at 120 mtorr, and fresh spectroscopic graphite surfaces were exposed to an argon plasma discharge at a current of 15 mA in an etching mode over time intervals ranging from 0 to 60 min. For other sets of experiments, the pressure was varied from 120 to 300 mtorr, and the discharge current from 5 to 45 mA. The contamination of the argon plasma (e.g. O_2 and others contaminants) was possible below a pressure of 120 mtorr and consequently, a minimum pressure value of 120 mtorr was considered.

Silver epoxy (EPO-TEK H20E, Epoxy Techn., Inc) was used to ensure good electrical contact. One face and the sides of the electrodes were coated with Epofix resin (Struers) to obtain a projected geometric surface area of 0.3 cm^2. Epofix resin, known for its stability (i.e. no leaching) in alkaline solutions, was used successfully in previous work to characterize electrode behaviour [14].

2.2. *Electrochemical measurements*

The electrochemical measurements for the HER were performed in a double-wall Pyrex glass cell in which the anodic and cathodic compartments were separated by a Nafion® membrane (Nafion® 901, Electrosynthesis Co.). The electrolysis was carried out at 25 °C in 1 M KOH (BDH 99.9%) prepared using deionized water (Barnstead Nanopure water with 17.5 mΩ resistivity). A pure platinum grid was used as the counter electrode; a Hg/HgO/1 M KOH reference electrode was connected to the cathodic compartment by a Luggin capillary. The measured value of the HER reversible potential in 1 M KOH was −925 mV with respect to the reference electrode. Nitrogen was bubbled through the solution prior and during electrolysis. The measurements were performed using a PAR model 273A potentiostat/galvanostat, PAR model 5210 two-phase lock-in analyser and Commodore PC2 microcomputer. A constant cathodic current of 33 mA cm^{-2} was applied for 30 min and the Tafel curve was recorded galvanostatically from 41 mA cm^{-2} to 0.01 μA cm^{-2}. The overpotentials were corrected for the ohmic drop using the a.c. impedance technique. The above procedure has been used for the characterization of the electrode materials for the HER [15, 16]; the procedure was repeated until no differences were observed in the cathodic polarization curves (after about three consecutive cycles). Once the Tafel curve was recorded, the a.c. measurements were carried out on the electrodes. The spectra were recorded in a frequency range from 10^4 to 0.1 Hz using 5 mV peak-to-peak amplitude. The selected applied d.c. potentials were located in the linear portion of the Tafel lines.

3. Results and discussion

3.1. *Effect of etching time during the etching process*

As previously noted, spectroscopic graphite surfaces were etched for 0, 5, 15, 30, 45 and 60 min with a discharge current of 15 mA and a pressure of 120 mtorr to correlate the effects of argon plasma etching time on the electrocatalytic activity of the electrode materials for HER. The log(*i*) against hydrogen overpotential (η_{H_2}) curves are given in Fig. 1 for the different ETs under consideration. The following has been deduced from the Fig. 1 curves: (i) the log(*i*) versus the η_{H_2} curves are practically linear relationships, with the Tafel parameters given under Fig. 1 for each ET, (ii) the HER electrocatalytic activity has improved from 0 to 30 min of ET to further decrease for larger ETs and (iii) the Tafel slope increases from 0 to 5 min of ET to be practically con-

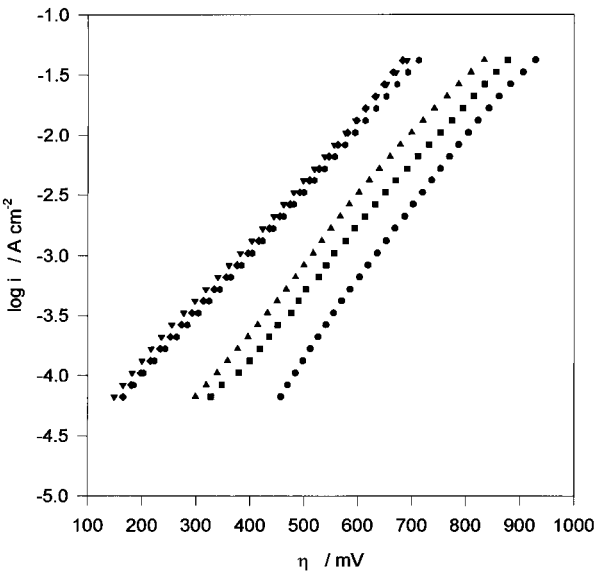

Fig. 1. Tafel plots for spectroscopic graphite electrodes for ET of 0 (●), 5 (■), 15 (▲), 30 (▼), 45 (◆) and 60 min (⬢); (120 mtorr and 15 mA) in 1 M KOH at 25 °C. Tafel parameters: b = 167 mV dec^{-1}, j_0 = 0.15 μA cm^{-2} for ET = 0 min; b = 191 mV dec^{-1} j_0 = 1.15 μA cm^{-2} for ET = 5 min; b = 185 mV dec^{-1}, j_0 = 1.65 μA cm^{-2} for ET = 15 min; b = 197 mV dec^{-1}, j_0 = 11.8 μA cm^{-2} for ET = 30 min; b = 189 mV dec^{-1}, j_0 = 8.45 μA cm^{-2} for ET = 45 min; b = 195 mV dec^{-1}, j_0 = 8.90 μA cm^{-2} for ET = 60 min.

stant from 5 to 60 min of ET. It is relevant to note that the HER rate jumps by a factor of about 40 from ET = 0 to ET = 30 min in the potential region ranging from 350 to 600 mV.

The a.c. impedance spectroscopy was used to clarify the HER for different ETs. Typical complex-plane diagrams are shown in Fig. 2 for electrodes with an ET of 30 min and η_{H_2} ranging from 342 to 537 mV. Only one semicircle is noticed for all potential values; the larger η_{H_2}, the lower the charge transfer resistance. The points correspond to the experimental data and the lines to the constant-phase element (CPE) model simulation using the fitting program written by MacDonald [17]. The Fig. 3 Bode curves also show that very good fits are obtained for all experimental sets of data. The surface roughness factor induces frequency dispersion due to nonuniform distribution of current density. Over a wide range of frequencies such effects may be accounted for with the empirical CPE model [18]. The double-layer capacitance, C_{dl}, was calculated from the a.c. impedance data for different η_{H_2} values and ETs of 0, 15, 30 and 45 min according to the fitting simulations, with detailed calculations provided in [19]. C_{dl} values are expressed against η_{H_2} in Fig. 4. C_{dl} is linked to both η_{H_2} and ET. At any overpotential value, the lowest C_{dl} is observed for an ET of 0 min and the highest C_{dl}, for an ET of 30 min; it is also noted that C_{dl} increases with an ET of up to 30 min to further decrease with an ET ranging from 30 to 45 min. Such an increase of C_{dl} with ET was already found [10] for HOPG substrates under similar experimental conditions. The comparison of C_{dl} for the same ET between HOPG and spectroscopic graphite surfaces shows that the values of C_{dl} are higher in the latter case. This is ascribed to the porous nature of spectroscopic graphite compared to HOPG.

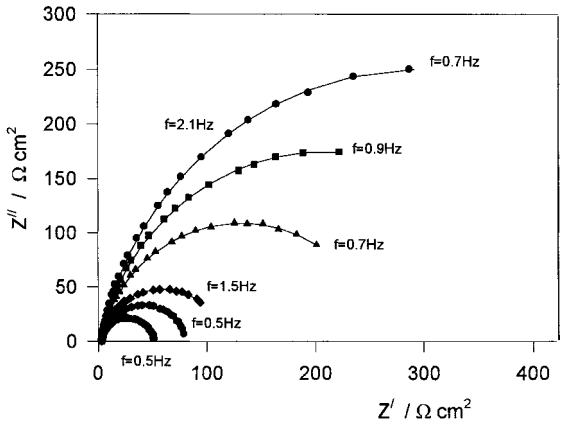

Fig. 2. Complex plan plots obtained on spectroscopic graphite etched for 30 min (120 mtorr and 15 mA) in 1 M KOH at 25 °C. Points: experimental values, lines: calculated values according to the CPE model. Key: (●) 342, (■) 380, (▲) 416, (◆) 479, (⬢) 508 and (●) 537 mV.

Surface modifications induced by argon plasma etching were investigated by SEM analysis. Before etching, a surface morphology characteristic of pressed-graphite powder is noted. Up to an ET of 30 min, as the argon plasma etching is processing, new features are noticed for the surface morphology, a longer ET, and a finer surface morphology, due to the formation of small cone-like peaks (Fig. 5); the height of these peaks is about 0.1–1.0 μm. Further, it is deducted that the erosion process occurs mainly at the crest of the pressed-graphite particles because there is more exposure.

The charge transfer resistance obtained from a.c. impedance measurements, together with the associated Tafel plots, was used in order to determine the easiest pathway for the HER. It is well established that the HER in alkaline solutions can proceed through any of the following reactions:

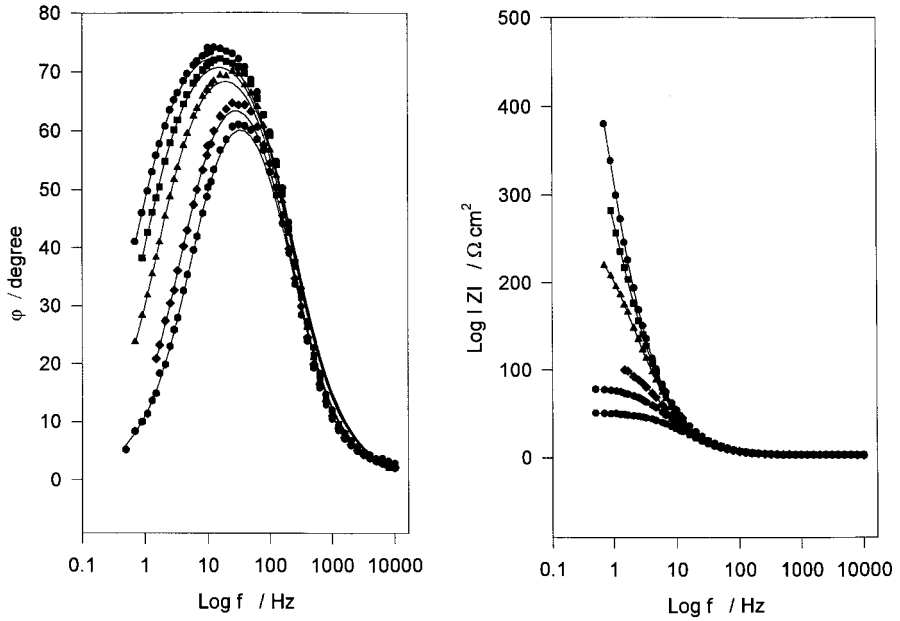

Fig. 3. Bode plots obtained on spectroscopic graphite etched for 30 min (120 mtorr and 15 mA) in 1 M KOH at 25 °C. Points: experimental values, lines: calculated values according to the CPE model. Key: (●) 342, (■) 380, (▲) 416, (◆) 479, (⬢) 508 and (●) 537 mV.

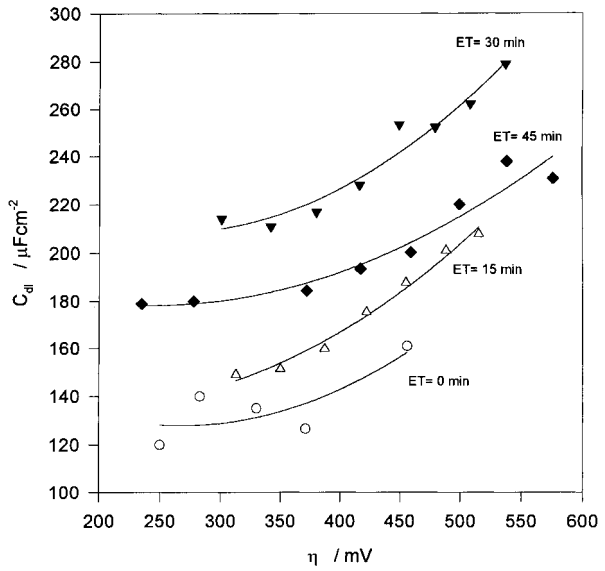

Fig. 4. Dependence of the double-layer capacitance of spectroscopic graphite electrode on overvoltage in 1 M KOH solution at 25 °C for different etching times.

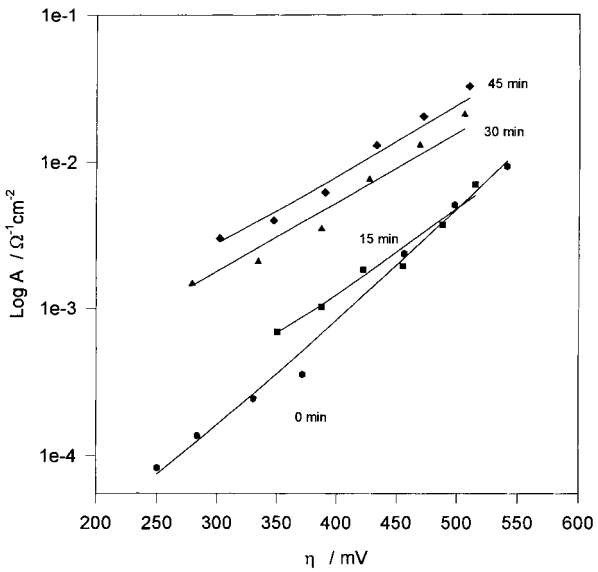

Fig. 6. Dependence of log A against HER overpotential for spectroscopic graphite electrodes etched during 0, 15, 30 and 45 min (120 mtorr and 15 mA). Points: experimental values, lines: calculated values according to the Volmer–Heyrovsky mechanism.

$$H_2O + M + e^- = MH_{ads} + OH^- \quad k_1, k_{-1} \quad \text{(Volmer reaction)} \quad (1)$$

$$H_2O + MH_{ads} + e^- = M + H_2 + OH^- \quad k_2, k_{-2} \quad \text{(Heyrovsky reaction)} \quad (2)$$

$$2MH_{ads} = 2M + H_2 \quad k_3, k_{-3} \quad \text{(Tafel reaction)} \quad (3)$$

where k_i represents the rate constant of the forward (+) and backward (−) processes. Water reduction with hydrogen adsorption (Reaction 1) is followed by electrochemical and/or chemical desorption (Reactions 2 and 3, respectively). In the present investigation, it was found that the best approximation of the experimental data with the theoretical model (i.e. the easiest pathway for the HER) corresponds to the Volmer–Heyrovsky (V–H) reaction. The experimental values of the charge transfer resistance and the associated simulated curves are illustrated in Fig. 6 for electrodes made of spectroscopic graphite having experienced argon plasma etching. The V–H pathway is commonly observed in alkaline media for some electrode materials [19]. The kinetic parameters of the HER rate-determining step (r.d.s.) (the Volmer reaction), are summarized in Table 2 for electrodes with different ETs. The parameters for the Heyrovsky reaction are not given because $k_2 \gg k_1$ and the associated errors on k_2 were larger than the values of k_2. It should be noted that the rate constant value of the r.d.s. for spectroscopic graphite electrodes is ET-dependent, longer ET, larger k_1. k_1 was divided by the surface roughness factor (R_f) in order to estimate the intrinsic electrode activity [19]. Assuming that the capacitance of the basal plane for a freshly cleaved HOPG electrode is about 3 μF cm^{-2} [20], R_f corresponds to C_{dl} (μF cm^{-2})/3 (μF cm^{-2}). Table 2 summarizes the intrinsic rate constant values. It is deduced that the intrinsic activity of the spectroscopic

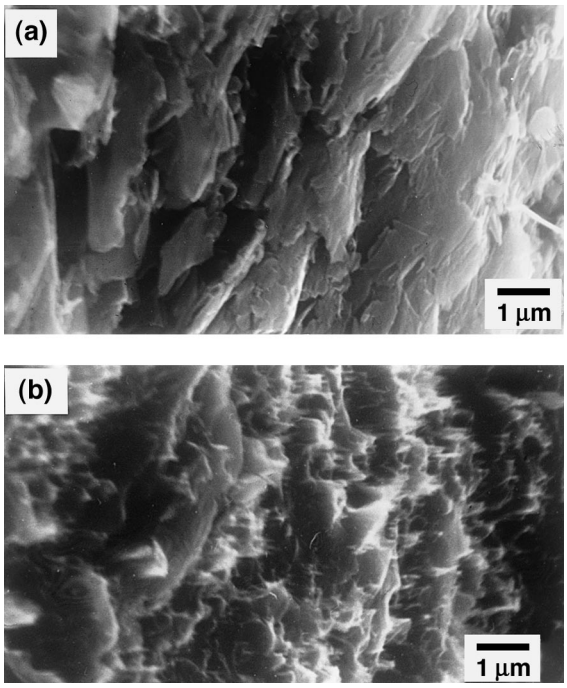

Fig. 5. SEM pictures of a spectroscopic graphite electrode (×6 500, inclined view 65°): (a) for a fresh electrode, (b) for ET = 15 min.

Table 2. HER kinetic parameters for composite-coated electrodes in 1 M KOH at 25 °C using the Volmer–Heyrovsky reaction mechanism

Etching time /min	$10^{12}k_1$ /mol cm^{-2}s^{-1}	α_1	R_f	$10^{14}k_1/R_f$ /mol cm^{-2} s^{-1}
0	0.25	0.36	46	0.54
15	1.28	0.36	50	2.56
30	16.50	0.28	71	22.75
45	17.90	0.30	60	29.00

graphite surface is increased by the argon bombardment etching, that is, the HER electrocatalytic activation induced by the ionic bombardment is not due to a geometric effect only. As already mentioned, electrocatalytic enhancement of graphite electrodes as a result of surface modifications other than an increase in the roughness factor increase may be linked to various phenomena such as the removal of contaminants, exposure of microparticles, defects, and fresh edge planes that may be preferred sites for the electron transfer. It is interesting to note that several studies on pyrolytic graphite electrodes for HER in acidic solutions [21, 22] have shown strong differences between edges and basal planes as far as electrocatalytic activity is concerned. However, in the present case, the origin of the intrinsic activity increase remains to be determined and requires further investigation.

3.2. *Effect of the discharge current during the etching process*

Spectroscopic graphite surfaces were etched under different discharge currents for sustaining the plasma, the other experimental conditions remaining unchanged, that is, ET of 15 min and the applied pressure of 120 mtorr. The Tafel plots for HER on electrodes etched at a discharge current of 5, 15 and 45 mA are illustrated on Fig. 7, with the Tafel parameters given under for each curve. It is noticed that the Tafel slope for an electrode etched with a discharge current of 15 mA is significantly lower compared to the values obtained for electrodes etched at 5 and 45 mA. For $\eta > 400$ mV, HER electrocatalytic activity is at its maximum for a discharge current of 15 mA. The latter observation is consistent with the fact that increasing the discharge current leads to a higher density of ionized argon in the incident flux. Consequently, more particles impinge the surface for a given time. It is equivalent to maintaining the discharge current constant and increasing the etching time. However, as shown above, there is a critical value for the time beyond which the etching process has a negative influence on electrode activity. The same phenomenon seems to be predominant with the current effect.

3.3. *Effect of the applied pressure during the etching process*

Pressure in the etching chamber ranged from 120 to 300 mtorr, with the discharge current maintained at 15 mA with ET of 15 min. Figure 8 exhibits the Tafel plots. It is noted that a maximum HER electrocatalytic activity is obtained for 120 mtorr and that the Tafel slope increases from 120 to 300 mtorr.

The lower electrode activity with a higher applied pressure above 120 mtorr may be explained by the sputtering erosion [23]. Increasing the pressure gives rise to a higher number of collisions between ions and neutral gas atoms and decreases the efficiency of the plasma, resulting in a higher number of bombardments with particles having an average energy that is often less than 10% of the applied potential [24]. Consequently, the erosion process is less efficient thus leading to a lower electrocatalytic activation.

4. Conclusion

The electrocatalytic activity of spectroscopic graphite surfaces was improved for the HER by using argon plasma etching. It has been shown that this surface

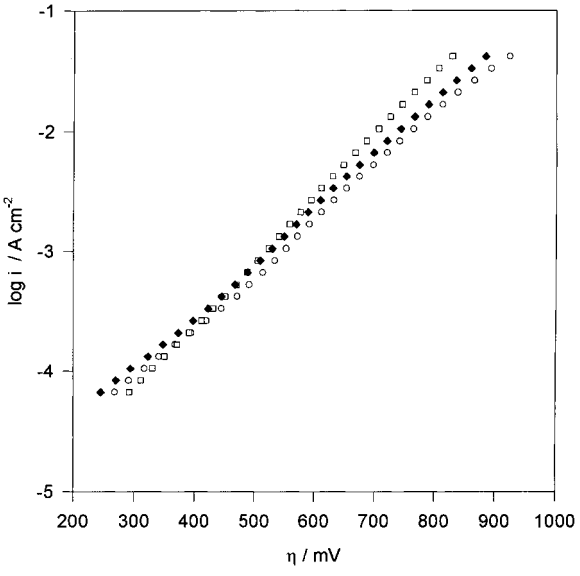

Fig. 7. Tafel plots for spectroscopic graphite electrodes for a discharge current of 5 (○), 15 (□) and 45 mA (◆), (120 mtorr and ET = 15 min). Tafel parameters: $b = 225\,\text{mV dec}^{-1}$, $j_0 = 3.94\,\mu\text{A cm}^{-2}$ for a discharge current of 5 mA; $b = 185\,\text{mV dec}^{-1}$, $j_0 = 1.64\,\mu\text{A cm}^{-2}$ for a discharge current of 15 mA; $b = 223\,\text{mV dec}^{-1}$, $j_0 = 4.56\,\mu\text{A cm}^{-2}$ for a discharge current of 45 mA.

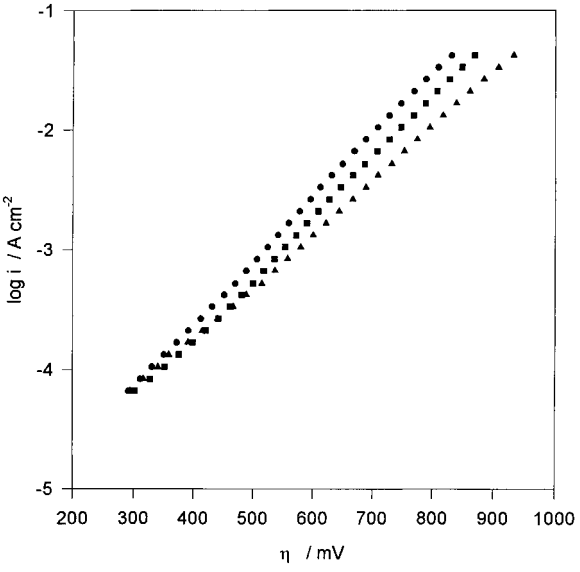

Fig. 8. Tafel plots for spectroscopic graphite electrodes and an applied pressure of 120 (●), 200 (■) and 300 mtorr (▲), (current discharge of 15 mA and ET = 15 min). Tafel parameters are $b = 185\,\text{mV dec}^{-1}$, $j_0 = 1.65\,\mu\text{A cm}^{-2}$ for an applied pressure of 120 mtorr; $b = 197\,\text{mV dec}^{-1}$, $j_0 = 1.61\,\mu\text{A cm}^{-2}$ for an applied pressure of 200 mtorr; $b = 225\,\text{mV dec}^{-1}$, $j_0 = 2.96\,\mu\text{A cm}^{-2}$ for an applied pressure of 300 mtorr.

pretreatment leads to a significant increase of the HER rate at a given overpotential value. Further, it has been shown that induced modifications on the electrode surface are such that they give rise to intrinsic electrocatalytic activity together with an increase in surface roughness. Finally, it has been shown that the experimental conditions used for sustaining the plasma such as argon pressure and working current play an important role for the treatment efficiency for the electrode activation toward HER.

Acknowledgements

Special thanks go to Dr B. Mahdavi (LTEE, Shawinigan (QUE), Canada) for his helpful comments. The financial support of the National Research Council of Canada and Hydro-Québec (IREQ) is gratefully acknowledged.

References

[1] K. Kinoshita, in Carbon, 'Electrochemical and Physicochemical Properties' (edited by K. Kinoshita) J. Wiley & Sons, New York (1988), p. 251.
[2] I. Hu, D. H. Karweik and T. Kuwana, *J. Electroanal. Chem.* **188** (1985) 59.
[3] R. J. Taylor and A. A. Humffray, *ibid.* **42** (1973) 347.
[4] K. J. Stutts, P. M. Kovach, W. G. Kuhr and R. M. Wightman, *Anal. Chem.* **55** (1983) 1632.
[5] R. C. Engstrom and V. A. Strasser, *Anal. Chem.* **56** (1984) 136.
[6] Mc Creery, in 'Electroanalytical Chemistry' (edited by A. J. Bard), Vol. 17 (1991), p. 222.
[7] H. You, N. Brown and K. F. Al-Assadi, *Surf. Sci.* **284** (1993) 263.
[8] E. A. Eklund, E. J. Snyder and R. S. Williams, *ibid.* **285** (1993) 157.
[9] J. R. Randin, in 'Encyclopedia of Electrochemistry of the Elements' Vol. 7 (edited by A. J. Bard), Marcel Dekker, New York (1976), p. 21.
[10] J. Fournier, D. Miousse, L. Brossard and H. Ménard, *Mat. Chem. Phy.* **42** (1995) 181.
[11] P. Dabo, B. Mahdavi, H. Ménard and J. Lessard, *Electrochim. Acta* **42** (1997) 1457.
[12] A. M. Couper, D. Pletcher and F. C. Walsh, *Chem. Rev.* **90** (1990) 837.
[13] K. Kinoshita, in 'Carbon: Electrochemical and Physicochemical Properties' (edited by K. Kinoshita) J. Wiley & Sons, New York (1988), p. 32.
[14] P. K. Wrona, A. Lasia, M. Lessard and H. Ménard, *Electrochim. Acta* **37** (1992) 1283.
[15] E. Potvin, A. Lasia, H. Ménard and L. Brossard, *J. Electrochem. Soc.* **138** (1991) 900.
[16] J. Borodzinski and A. Lasia, *J. Appl. Electrochem.* **24** (1994) 1267.
[17] J. R. Macdonald, J. Schoonman and A. P. Lehner, *J. Electroanal. Chem.* **131** (1982) 77.
[18] G. J. Brug, A. L. G. van Der Eeden, M. Sluyters-Rehbach and J. H. Sluyters, *ibid.* **176** (1984) 275.
[19] A. Lasia, in *Curr. Top. Electrochem., Research Trends* **2** (1993) 239.
[20] K. Kinoshita, in 'Carbon: Electrochemical and Physicochemical Properties' (edited by K. Kinoshita) J. Wiley & Sons, New York (1988), p. 293.
[21] M. P. J. Brennan and O. R. Brown, *J. Appl. Electrochem.* **2** (1972) 43.
[22] A. R. Despic, D. M. Drzic, G. A. Savic-Maglic and R. T. Atanasoski, *Croat. Chem. Acta.* **44** (1972) 79.
[23] J. A. Thornton, in 'Deposition Technologies for Films and Coatings' (edited by R. F. Bunshah), Noyes Publications, New Jersey, Chap. 5, p. 191.
[24] W. D. Davis and T. A. Vanderslice, *Phys. Rev.* **131** (1963) 219.